β3 Integrin–EGF receptor cross-talk activates p190RhoGAP in mouse mammary gland epithelial cells

Nikolas Balanis[a], Masaaki Yoshigi[b], Michael K. Wendt[c], William P. Schiemann[c], and Cathleen R. Carlin[a,c,d]

[a]Department of Physiology and Biophysics, Case Western Reserve University, Cleveland, OH 44106; [b]Department of Pediatrics, University of Utah, Salt Lake City, UT 84132; [c]Case Western Reserve University Comprehensive Cancer Center and [d]Department of Molecular Biology and Microbiology, Case Western Reserve University, Cleveland, OH 44106

ABSTRACT **Active RhoA localizes to plasma membrane, where it stimulates formation of focal adhesions and stress fibers. RhoA activity is inhibited by p190RhoGAP following integrin-mediated cell attachment to allow sampling of new adhesive environments. p190RhoGAP is itself activated by Src-dependent tyrosine phosphorylation, which facilitates complex formation with p120RasGAP. This complex then translocates to the cell surface, where p190RhoGAP down-regulates RhoA. Here we demonstrate that the epidermal growth factor receptor (EGFR) cooperates with β3 integrin to regulate p190RhoGAP activity in mouse mammary gland epithelial cells. Adhesion to fibronectin stimulates tyrosine phosphorylation of the EGFR in the absence of receptor ligands. Use of a dominant inhibitory EGFR mutant demonstrates that fibronectin-activated EGFR recruits p120RasGAP to the cell periphery. Expression of an inactive β3 integrin subunit abolishes p190RhoGAP tyrosine phosphorylation, demonstrating a mechanistic link between β3 integrin–activated Src and EGFR regulation of the RhoA inhibitor. The β3 integrin/EGFR pathway also has a positive role in formation of filopodia. Together our data suggest that EGFR constitutes an important intrinsic migratory cue since fibronectin is a key component of the microenvironment in normal mammary gland development and breast cancer. Our data also suggest that EGFR expressed at high levels has a role in eliciting cell shape changes associated with epithelial-to-mesenchymal transition.**

Monitoring Editor
Josephine Clare Adams
University of Bristol

Received: Aug 16, 2010
Revised: Sep 7, 2011
Accepted: Sep 12, 2011

INTRODUCTION

Multicellular organisms rely on cell migration throughout their life span. Cells specified in one region of the embryo migrate over long distances to form functionally distinct tissues (Keller, 2005; Aman and Piotrowski, 2010). Cell migration facilitates repair mechanisms in the adult notably during wound healing, when fibroblasts and inflammatory cells migrate to sites of injury (Barrientos *et al.*, 2008). Cell migration is also important in organs such as mammary glands that restructure epithelial tissues during morphogenesis (Pozzi and Zent, 2011). Cells become invasive and undergo metastasis when migration processes involved in epithelial morphogenesis are reactivated in solid human tumors (Wels *et al.*, 2008; Gray *et al.*, 2010). Despite major advances in therapies that curb tumor growth, metastatic disease has proven difficult to control (Wittekind, 2005; Sleeman and Steeg, 2010). Metastasis is the leading cause of death in cancer patients, underscoring the importance of understanding fundamental cell migration mechanisms.

The extension of the plasma membrane is one of the first steps in cell migration (Borisy and Svitkina, 2000; Pollard and Borisy, 2003). Animal cells produce membrane protrusions such as lamellipodia

This article was published online ahead of print in MBoC in Press (http://www.molbiolcell.org/cgi/doi/10.1091/mbc.E10-08-0700) on September 21, 2011.

Address correspondence to: Cathleen Carlin (cathleen.carlin@case.edu).

Abbreviations used: CaLB, Ca^{2+}-dependent phospholipid binding; ECM, extracellular matrix; EGFR, epidermal growth factor receptor; EMT, epithelial-to-mesenchymal transition; FAK, focal adhesion kinase; FN, fibronectin; GAP, GTP–GDP exchange activating protein; IL2Rα, interleukin 2 receptor α subunit; NMuMG, normal murine mammary gland; PH, pleckstrin homology; RBD, Rho GTPase binding domain; TNBC, triple-negative breast cancer; WT, wild type.

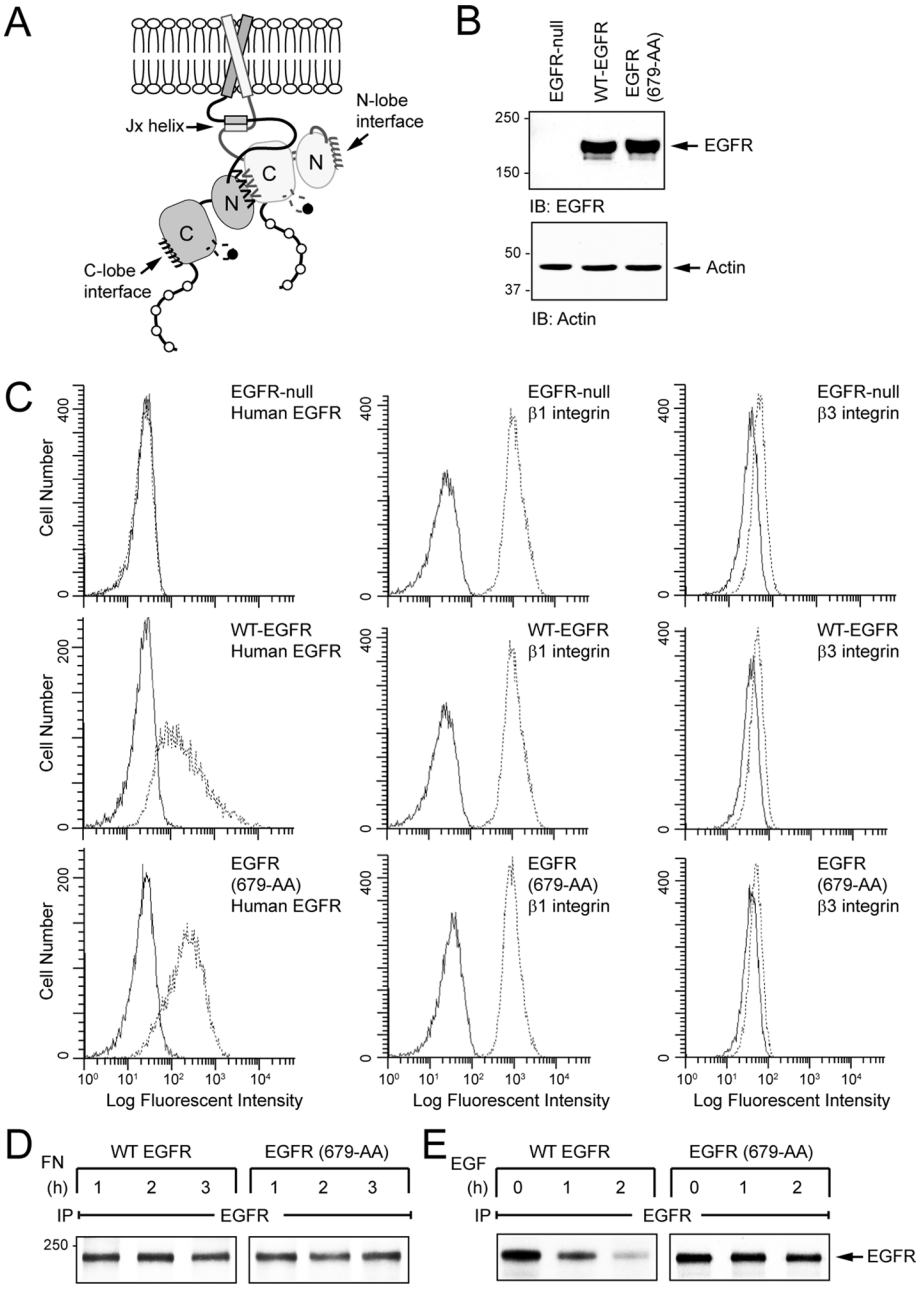

FIGURE 1: Reconstituted EGFR does not alter FN integrin cell surface expression in EGFR-null fibroblasts. (A) Model depicting interactions between EGFR cytosolic tail sequences leading to allosteric kinase activation in ligand-induced asymmetric dimers [adapted from Hubbard (2009)]. The C-terminal lobe of one kinase domain (light gray) interacts with the N-terminal domain of a second kinase domain (dark gray) via critical residues located at the dimer interface [depicted as uuuu (unoccupied) or vvvv (occupied)]. The 679-LL lysosomal sorting signal maps to the N-terminal lobe dimer interface (Kil *et al.*, 1999). Sequences in adjacent juxtamembrane (Jx) regions form an antiparallel amphipathic helix that facilitates dimerization (Jura *et al.*, 2009). Tyrosine residues that undergo auto- or Src-dependent phosphorylation (open or black circles, respectively) and activation loops (dashed lines) are also depicted. (B) Equal protein aliquots were immunoblotted with specific antibodies listed in the figure. (C) Histograms for cell surface expression of EGFR and FN integrins detected by flow cytometry (dashed lines) vs. background fluorescence associated with secondary antibodies (solid lines). The *y*-axis represents cell number, and the *x*-axis is fluorescence intensity on a logarithmic scale. Flow experiments were repeated at least twice. (D, E) Cells were metabolically labeled with ^{35}S-labeled amino acids for 30 min, followed by a 3-h chase. Cells were either adhered to FN (D) or stimulated with EGF (E) for times indicated. EGFR immune complexes were resolved by SDS–PAGE, and radioactive proteins were detected by fluorography.

and filopodia through coordinated action of actin cytoskeleton, cell adhesions, and plasma membrane (Condeelis, 1997). Lamellipodia are broad, thin membrane protrusions with a dendritic network of branched actin filaments abutting the plasma membrane that generate motile force through a combination of plus-end actin polymerization, retrograde flow, and cell adhesion (Petri *et al.*, 2009). Filopodia are finger-like membrane projections filled with bundles of parallel actin filaments (Mattila and Lappalainen, 2008). Although they are not absolutely required for cell migration, cells use filopodia to explore their environment and form new adhesive contacts for motility and spreading (Rorth, 2003; Gupton and Gertler, 2007). Filopodia have also been implicated in conveying long-distance signals important for pattern formation in developing epithelia (Cohen *et al.*, 2011). Most cultured cells produce both organelles upon initial contact with extracellular matrix (ECM).

Actin cytoskeleton and ECM are physically connected via cell adhesions initiated by activation of integrin transmembrane receptors (Hynes, 2002). Signaling receptors such as the epidermal growth factor receptor (EGFR) modulate normal cell behavior by forming physical and functional complexes with integrins that bind fibronectin (FN; Moro *et al.*, 2002; Marcoux and Vuori, 2003). Elevated EGFR expression contributes to carcinoma development and metastasis by stimulating proliferation and enhancing survival of FN-attached cells in the absence of ligand (Bill *et al.*, 2004; Muller *et al.*, 2009). EGFR also affects tumor angiogenesis by modifying branching behavior in endothelial cells within the tumor microenvironment (De Luca *et al.*, 2008). Previous studies indicate that elevated EGFR expression is sufficient to transform normal mammary epithelial cells similar to polyoma middle T using the normal murine mammary gland (NMuMG) cell model (Wendt *et al.*, 2010). These same studies showed that elevated EGFR expression enhances mesenchymal characteristics induced by EGF or transforming growth factor (TGF)-β and also primes NMuMG cells for TGF-β–driven epithelial-to-mesenchymal transition (EMT). Although integrin–EGFR signaling is implicated in multiple cell migration pathways, relatively little is known about its involvement in the formation of motile membrane protrusions in normal and pathological settings (Moro *et al.*, 2002; Marcoux and Vuori, 2003; Tran *et al.*, 2004).

Ligand-induced EGFR activation involves formation of asymmetric dimers between adjacent tyrosine kinase domains (Figure 1A) (Zhang *et al.*, 2006). This mode of activation

is regulated by residues that form a flexible interface between the C-terminal lobe of one tyrosine kinase domain and the N-terminal lobe of its dimer partner (Figure 1A). The intracellular EGFR juxtamembrane region plays a crucial role in stabilizing these asymmetric dimers (Jura *et al.*, 2009; Red Brewer *et al.*, 2009). Residues in the juxtamembrane region and dimer interface modulate a number of other functions, suggesting they integrate EGFR activation with cellular responses (Hunter and Cooper, 1985; Countaway *et al.*, 1989; Cochet *et al.*, 1991; Martin-Nieto and Villalobo, 1998; Ryan *et al.*, 2010). Residues Leu-679 and Leu-680 (679-LL) located in the N-terminal lobe interface regulate postendocytic sorting to lysosomes (Kil *et al.*, 1999; Kil and Carlin, 2000). Receptors with a 679–amino acid dialanine substitution (EGFR (679-AA)) undergo ligand-accelerated internalization similar to wild-type EGFR (WT-EGFR) but are routed away from lysosomes to a recycling pathway, where they are coupled to novel signaling complexes (Kostenko *et al.*, 2006). These findings provide new insights into signaling pathways up-regulated in breast cancer cell lines, where EGFR forms dimers with related ErbB family members that divert activated EGFRs to recycling endosomes similar to EGFR (679-AA) (Yarden and Sliwkowski, 2001; Wiley, 2003; Kostenko *et al.*, 2006). The role of these residues during EGFR transactivation independent of growth factor stimulation has not been addressed.

We demonstrate here that EGFR has a significant role in determining how both normal mouse mammary gland epithelial cells and those poised for EMT respond to FN-enriched adhesive environments. Our data support a model that signaling through β3 integrin FN receptors via EGFR activates the RhoA antagonist p190RhoGAP by recruiting its binding partner p120RasGAP to plasma membrane. We also provide evidence that the β3 integrin–EGFR pathway is a positive regulator of filopodia formation. EGFR with the 679–amino acid substitution had an instrumental role in dissecting this pathway since it behaves as a dominant inhibitory molecule capable of interfering with β3 integrin–EGFR signaling.

RESULTS

The 679-AA mutation selectively blocks tyrosine phosphorylation on a subset of EGFR residues in reconstituted EGFR-null cells

The overall goal of these studies was to determine the role of EGFR during the early stages of cell migration when cells form initial contacts with FN. Initial studies were carried out using human EGFR expressed in NR6 mouse fibroblastic cells, which lack endogenous receptor (Pruss and Herschman, 1977). This heterologous expression system was used previously to study effects of EGFR on cell morphology and motility (Welsh *et al.*, 1991; Chen *et al.*, 1994; Maheshwari *et al.*, 2000; Allen *et al.*, 2002; Chou *et al.*, 2003; Zhou *et al.*, 2006). NR6-derived cells are also suitable for studies with FN since they express both major forms of FN receptors ($\alpha_5\beta_1$ and $\alpha_v\beta_3$; Maheshwari *et al.*, 1999). In addition to WT-EGFR, cells reconstituted with EGFR (679-AA) were examined since this mutant had already yielded novel insights into ligand-induced EGFR activation (Kil *et al.*, 1999; Kil and Carlin, 2000). Reconstituted cell lines were selected with equivalent levels of total cellular and cell surface EGFR expression based on immunoblotting and flow cytometry, respectively, using human receptor–specific antibodies (Figure 1, B and C). Cells were also incubated with fluorescein isothiocyanate (FITC)–conjugated β1 or β_3 integrin antibodies and subsequently analyzed by flow cytometry to determine whether ectopic EGFR expression alters basal trafficking of FN integrins. All three cell lines expressed similar cell surface levels of both FN receptors, with β1 integrin expression relatively high compared with that of β3 integrin (Figure 1C). Furthermore, both EGFR proteins were biosynthetically stable up to 3 h postadhesion to FN, indicating cell adhesion does not route either receptor to lysosomes (Figure 1D). In contrast, WT-EGFR but not EGFR (679-AA) was rapidly degraded following ligand stimulation (Figure 1E), confirming the original EGFR (679-AA) phenotype (Kil *et al.*, 1999; Kil and Carlin, 2000).

We next asked whether WT-EGFR and EGFR (679-AA) were activated by FN binding. WT-EGFR was modified on a subset of tyrosine residues that also serve as major autophosphorylation sites after EGF stimulation (Tyr-992, Tyr-1068, and Tyr-1173; Figure 2A). In addition, WT-EGFR was phosphorylated on Tyr-845 (Figure 2A), a Src-specific substrate located in the activation loop in the tyrosine kinase domain (Figure 1A; Sato *et al.*, 1995; Biscardi *et al.*, 1999). EGFR (679-AA), however, was primarily phosphorylated at Tyr-992 in newly adherent cells (Figure 2A). Consistent with reports in the literature (Moro *et al.*, 2002; Playford and Schaller, 2004), EGFR and Src kinase inhibitors (AG1478 and PP2, respectively) interfered with FN-induced tyrosine phosphorylation of WT-EGFR and EGFR (679-AA) (Figure 2B). Furthermore, neither EGFR protein was activated by cell adhesion to collagen (Figure 2B), which also binds β1 integrin (Hynes, 2002), confirming that EGFR transactivation is FN specific in NR6 mouse fibroblasts.

Focal adhesion kinase (FAK) is a cytoplasmic protein tyrosine kinase involved in many aspects of integrin-mediated signal transduction, including cell spreading, migration, and survival (Hall *et al.*, 2011). Activation of FAK by integrin clustering leads to autophosphorylation at Tyr-397. We demonstrated that FAK was phosphorylated at Tyr-397 as a parallel readout of integrin activation in all three cell lines (Figure 2C). The multifunctional adaptor protein p130Cas is a prominent Src substrate that binds EGFR during FN-induced cell adhesion (Defilippi *et al.*, 2006). The p130Cas protein underwent rapid tyrosine phosphorylation in all three cell lines, confirming that endogenous Src is activated independent of EGFR expression (Figure 2D). Furthermore, p130Cas was phosphorylated on the same set of tyrosine residues in all cell lines, indicating that it forms similar molecular complexes (Figure 2D). Altogether these data suggest that 679-AA is a dominant inhibitory mutation that selectively modifies EGFR-specific cell adhesion responses without affecting other FN-induced pathways.

EGFR enhances membrane protrusive activity on FN

Preliminary studies indicated that all three cell lines were maximally spread on FN by 20 min (Supplemental Figure S1A). Cells adhered for 20 min (Figure 3, A–C) or 1 h (Supplemental Figure S1B) were stained with rhodamine-phalloidin to determine the effect of FN on morphology and F-actin cytoskeleton. Cells were costained with an antibody to vinculin, an adapter protein that localizes to integrin-mediated cell–matrix adhesions (Carisey and Ballestrem, 2011). The three cell lines displayed a spectrum of phenotypes that correlated with EGFR expression. EGFR-null cells exhibited a typical fibroblastic elongated shape with abundant parallel-ordered ventral actin stress fibers tethered at each end by prominent vinculin-positive focal adhesions (Figure 3A and Supplemental Figure S1B). Cells with WT-EGFR had prominent curved stress fibers, a network of cortical actin filaments abutting the plasma membrane, and multiple filopodial extensions around the entire periphery of the cell (Figure 3B and Supplemental Figure S1B). Vinculin was present on filopodial actin shafts in addition to the cell periphery (Figure 3B). Cells with WT-EGFR were also imaged by time-lapse microscopy starting ~10 min after FN seeding (Supplemental Videos A and B). Figure 3, D and E, shows sequential images of two cells with prominent filopodia that grow by extending from the cell periphery over a period of 60–120 s.

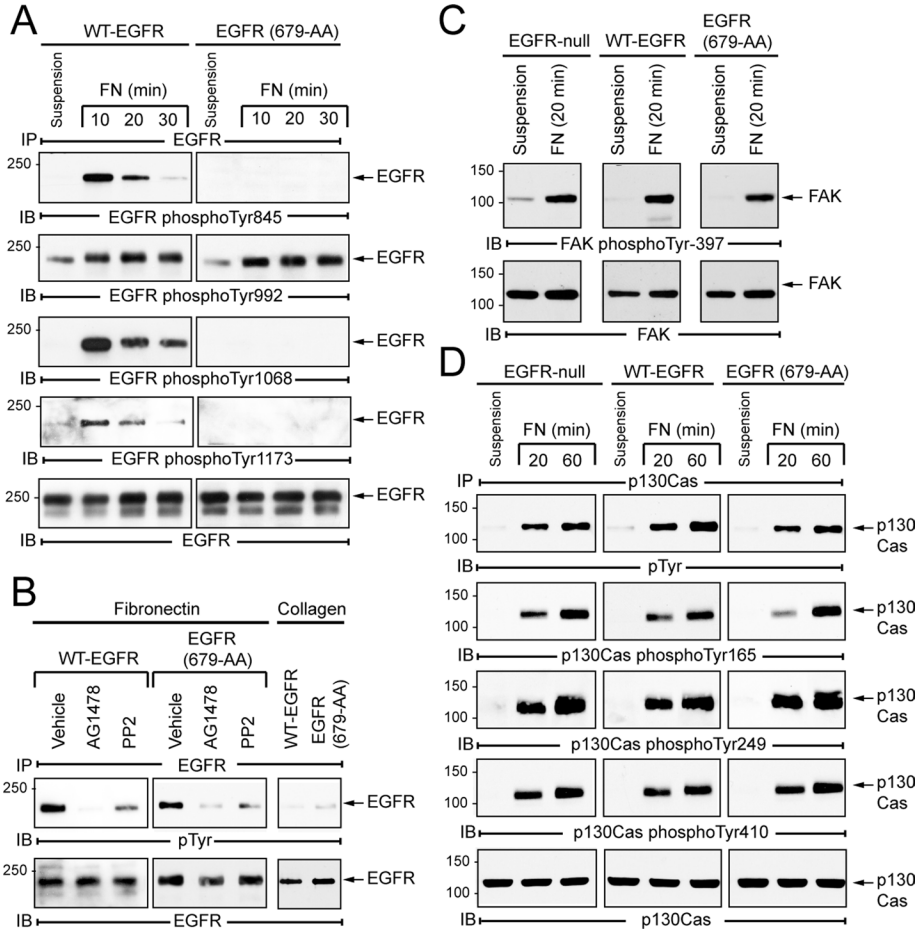

FIGURE 2: EGFR is transactivated by FN binding in mouse fibroblastic cell models. (A) EGFR immune complexes from suspended and FN-adhered cells were immunoblotted with phospho-specific EGFR antibodies listed in the figure. Bottom, immunoblotted with an activation-independent EGFR antibody. (B) Cells were pretreated with vehicle or EGFR (1 μM AG1478) or Src (10 μM PP2) tyrosine kinase inhibitors for 30 min and then adhered to FN or were adhered to collagen in the absence of kinase inhibitors. EGFR immune complexes were immunoblotted for phosphotyrosine (top). Blots were stripped and reprobed with an EGFR antibody to control for total protein loading (bottom). (C) Cells were adhered to FN for 20 min. Equal protein aliquots were immunoblotted with a phospho-specific antibody to activated FAK (top) or an antibody to total FAK protein (bottom). (D) p130Cas immune complexes from cells kept in suspension or adhered to FN for times indicated were immunoblotted with antibodies listed in the figure. (A–D) Representative of three (A, B) or two (C, D) independent experiments.

Cells with EGFR (679-AA) also lacked prominent ventral stress fibers. However, in contrast to WT-EGFR, cells with the mutant receptor had broad lamellipodial protrusions, giving them a more-rounded appearance, a dense ring of branching actin filaments associated with small, dot-like, vinculin-enriched focal adhesions located at the lamellum–lamellipodia border, and a sparse branching actin network in the lamellum (Figure 3C and Supplemental Figure S1B). Morphometric analysis showed that cells with WT-EGFR had a statistically significant fourfold increase in filopodia/cell compared with EGFR-null cells and a twofold to threefold increase compared with cells with EGFR (679-AA) (Figure 3F). Conversely, the mutant EGFR was associated with a twofold to threefold increase in the percentage of lamellipodial perimeter compared with WT-EGFR (Figure 3G).

To quantify adhesion-induced changes in stress fiber orientation, we adapted a previously described Sobel filter algorithm that measures stress fiber alignment of phalloidin-stained actin filaments (Yoshigi *et al.*, 2003). Individual cells were divided into pixel grids, and the angles of stress fibers in each grid were measured and binned to generate histograms of fiber orientation for individual cells (Figure 3, H–J). The kurtosis (i.e., peakedness) of angle distribution plots was determined for 100 cells and averaged to derive a relative stress fiber alignment index for each cell type. These analyses confirmed that the frequency of parallel-ordered stress fibers was significantly reduced in cells expressing WT-EGFR or EGFR (679-AA) compared with EGFR-null mouse fibroblasts (Supplemental Figure S1C). In contrast to FN, all three cell lines had similar phenotypes on collagen (Figure 3K). Collectively, these findings support two main conclusions. First, EGFR regulates either the type or mode of actin stress fiber formation on FN. Second, the 679-AA mutation interferes with a regulatory pathway associated with filopodia formation.

The 679-AA mutation interferes with FN-induced RhoA inhibition

Cell adhesion is frequently associated with an initial decline in RhoA activity (Ren *et al.*, 1999; Sander *et al.*, 1999). Experiments were carried out to determine whether this was also true in the heterologous EGFR expression system using enzyme-linked immunosorbent assay (ELISA)–based assays to measure GTP-bound Rho family members, which were expressed at similar levels in all three cell lines (Supplemental Figure S1D). Similar to EGFR-null cells, cells reconstituted with WT-EGFR exhibited a rapid decline in relative GTP-RhoA levels during the early stages of FN adhesion (Figure 4A; see Supplemental Table S1 for unadjusted absorbance data). However, cells with EGFR (679-AA) exhibited steady RhoA activity immediately following FN adhesion (Figure 4A). In contrast, all three cell lines displayed similar patterns of Rac1 (Figure 4B) and Cdc42 (unpublished data) activities on FN.

Previous studies showed that adhesion-induced inhibition of RhoA is mediated by Src-dependent tyrosine phosphorylation of p190RhoGAP necessary for its activation as a RhoA GTP–GDP exchange activating protein (GAP; Chang *et al.*, 1995; Arthur *et al.*, 2000; Roof *et al.*, 2000; Haskell *et al.*, 2001a, 2001b). p190RhoGAP also forms an active molecular complex with p120RasGAP (Hu and Settleman, 1997; Roof *et al.*, 1998). In addition to tyrosine phosphorylation and p120RasGAP complex formation, p190RhoGAP must be recruited to plasma membrane in order to be active (Bradley *et al.*, 2006). Because p120RasGAP is known to bind autophosphorylated EGFR (Trahey *et al.*, 1988; Wang *et al.*, 1996), we hypothesized that it might serve as a molecular link between FN-activated EGFR and p190RhoGAP. Coimmunoprecipitation studies revealed that p190RhoGAP formed a molecular complex with p120RasGAP in all three cell lines on FN (Figure 4C). Although p120RasGAP was also present in a complex with WT-EGFR after FN binding, the 679-AA mutation blocked this interaction (Figure 4D).

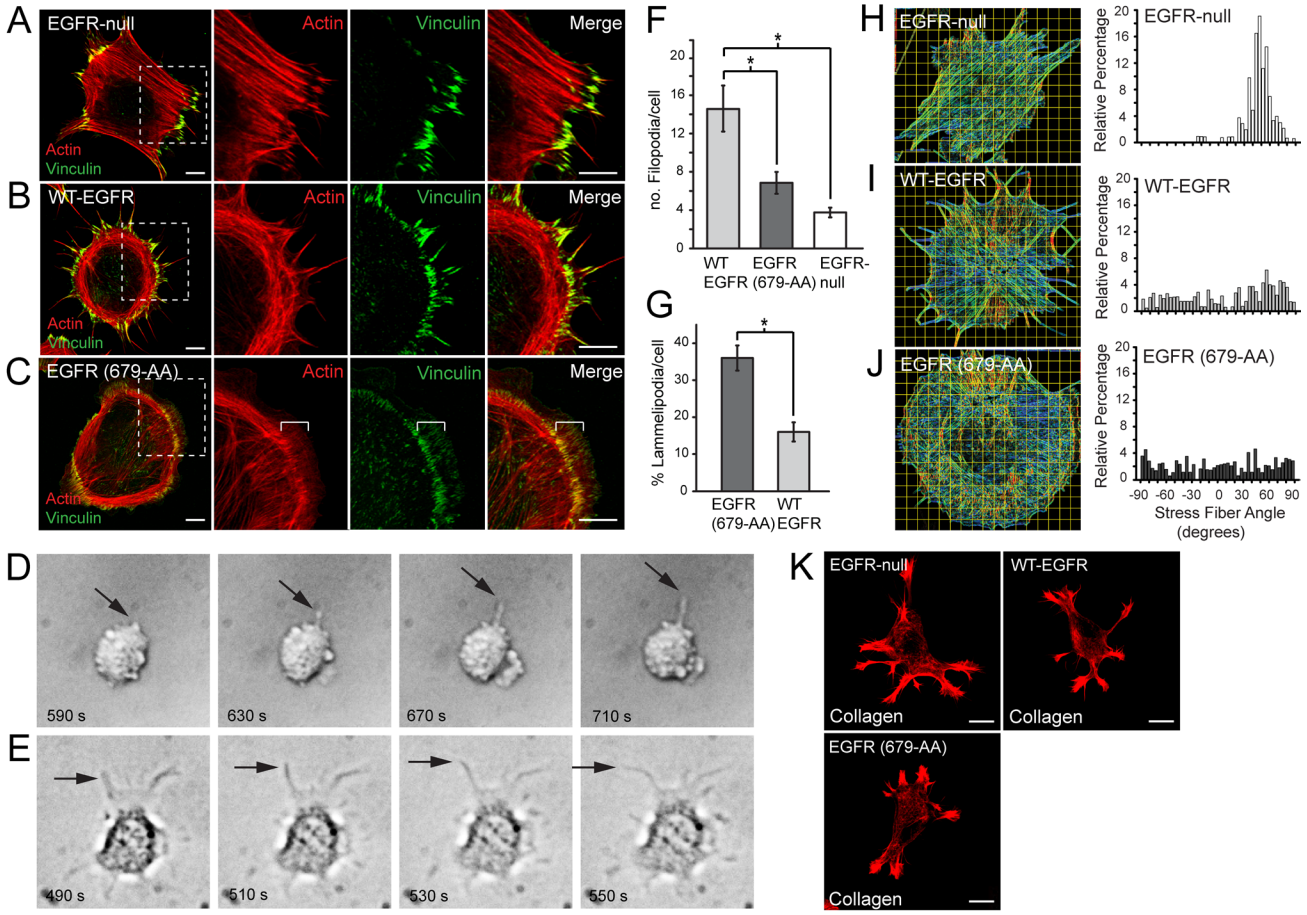

FIGURE 3: EGFR modulates FN-dependent cell morphology in mouse fibroblasts. (A–C) Confocal images of EGFR-null cells (A) and cells expressing WT-EGFR (B) or EGFR (679-AA) (C) adhered to FN for 20 min stained with phalloidin (red) to visualize actin cytoskeleton. Cells were also stained with a vinculin-specific antibody (green). Right, magnified images of boxed areas. Bracket, lamellum. (D, E) Time-lapse images of two cells expressing WT-EGFR starting 590 s (D) or 490 s (E) after FN seeding. Arrows point to thin structures consistent with filopodia. Images from Supplemental Videos A and B, respectively. (F, G) Bars represent the average number of filopodia/cell (mean ± SEM; n ≥ 60 cells) (F) or the average percentage of cell perimeter occupied by lamellipodial network/cell (mean ± SEM; n ≥ 60 cells from three independent experiments) (G). All measurements were made using phalloidin-stained images obtained 20 min postadhesion to FN. White bars, EGFR-null cells; light gray bars, cells with WT-EGFR cells; dark gray bars, cells with EGFR (679-AA). Asterisks indicate differences between cells that were statistically significant ($p < 0.001$) as determined by Student's *t* test. (H–J) Representative cell images for EGFR-null cells (H) and cells expressing WT-EGFR (I) or EGFR (679-AA) (J) divided into grids for analysis of stress fiber alignment. Stress fibers were color coded by remapping the fiber angle to the hue angle of HSV color space. This color coding shows vertical stress fibers in red and horizontal stress fibers in blue. Right, histograms of fiber orientation. The *x*-axis represents stress fiber angles from −90 to +90 deg. Stress fiber angles in individual grids were binned based on 4-deg intervals. The *y*-axis represents the relative percentage of grids with a specific bin designation. Mean kurtosis as an index of stress fiber alignment (mean ± SEM; n = 100 cells) corresponding to data in H, I, and J shown in Supplemental Figure S1C. (K) Confocal images of EGFR-null, WT-EGFR, or EGFR (679-AA) adhered to collagen for 20 min stained with phalloidin (red) to visualize actin cytoskeleton. Scale bars, A–C and K, 10 μm.

Surface coimmunoprecipitation studies were carried out to determine whether these molecular complexes were present at the cell surface. Newly adhered cells were incubated with EGFR1 antibody, which recognizes an extracellular human EGFR epitope, and cell lysates were then incubated with immunoglobulin G–affinity purification beads to capture EGFR immune complexes specifically formed at the cell surface. Control studies were carried out using an isoform-matched monoclonal antibody to the interleukin 2 receptor α subunit (IL2Rα). p120RasGAP was present in the same molecular complex as WT-EGFR but not EGFR (679-AA) (Figure 4E). In addition, WT-EGFR formed a complex with β3 integrin, in contrast to EGFR (679-AA), which was associated with β1 integrin at the cell surface (Figure 4E). β1 integrin also binds collagen. However, EGFR (679-AA) was not activated by collagen ligation (Figure 2B), and cells expressing the mutant receptor did not produce a discernible phenotype on collagen (Figure 3K), suggesting that the 679-AA mutation also interferes with collagen–EGFR signaling. We next tested the hypothesis that WT-EGFR causes p190RhoGAP to redistribute to membrane protrusions during cell adhesion, using confocal microscopy. The p190RhoGAP protein was concentrated in puncta that were overlapping or interspersed with EGFR-positive puncta along filopodial shafts in cells expressing WT-EGFR (Figure 4F; Figure 4, G and H, shows two additional examples of colocalized EGFR-p190RhoGAP on FN-induced filopodia). In

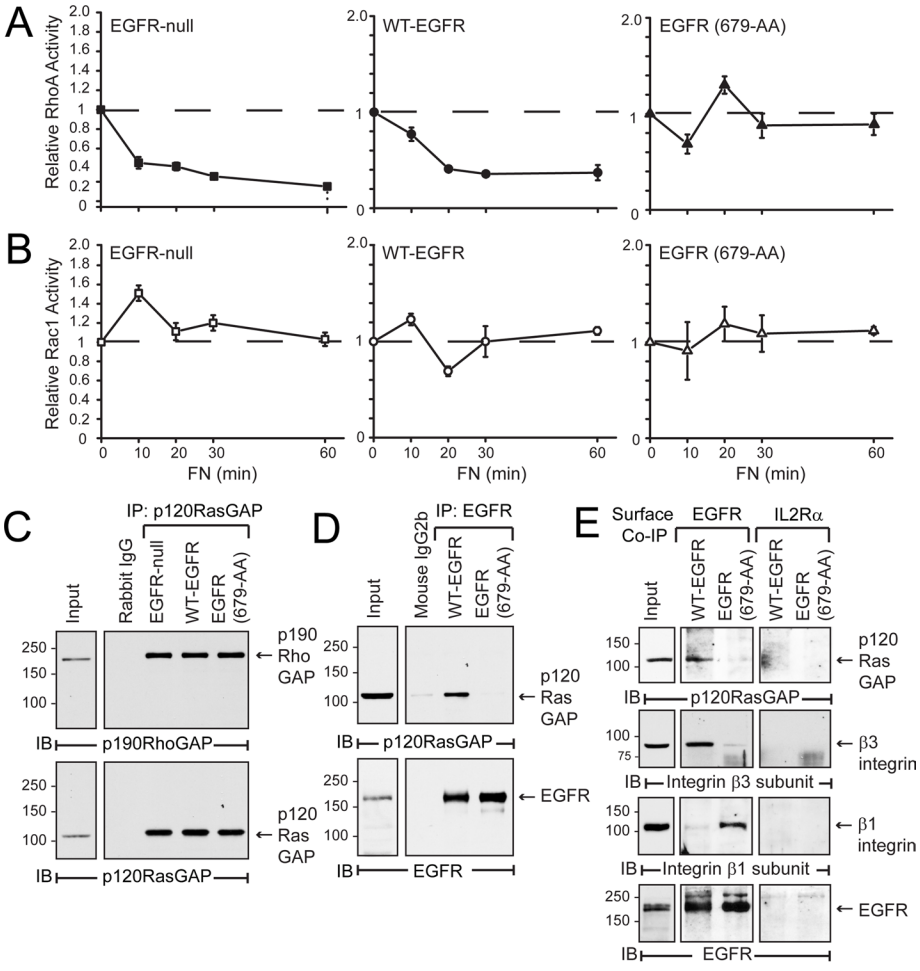

FIGURE 4: EGFR regulates p190RhoGAP activity. (A, B) Cells were kept in suspension or adhered to FN for times indicated, and GTPase activities were determined using RhoA-specific (A) or Rac1-specific (B) ELISAs. Data for cells in suspension were set to 1, and data from adherent cells were plotted as percentage change relative to 1 ± SEM (n = 3) as a function of time. See Supplemental Table S1 for unadjusted absorbance data. (C) The p120RasGAP immune complexes from cells adhered to FN for 20 min were immunoblotted with a p190RhoGAP antibody (top). Filters were stripped and reprobed with a second p120RasGAP to control for protein loading (bottom). Lysates were also immunoprecipitated with an irrelevant isotype-matched immunoglobulin G to control for nonspecific binding. Input lanes are aliquots of total cell protein set aside before immunoprecipitation. (D) EGFR immune complexes from cells adhered to FN for 20 min were immunoblotted with a p120RasGAP antibody (top) and reprobed with a second EGFR antibody (bottom). (E) Cells were incubated with an antibody to an extracellular human EGFR epitope or an isotype-matched negative control (IL2Rα antibody) as they were adhering to FN. Cells were harvested 20 min postadhesion, and immune complexes with membrane-exposed EGFRs were immunoblotted with an antibody to p120RasGAP. The same blot was stripped and successively reprobed with antibodies to β3 integrin, β1 integrin, and EGFR. Input lanes are aliquots of total cell protein set aside before immunoprecipitation. (C–E) Representative of three (C, D) or two (E) independent experiments. (F) Confocal images of cells with WT-EGFR adhered to FN for 20 min stained with phalloidin (green) and antibodies to EGFR (red) and p190RhoGAP (blue). Right, magnified images of individual and merged channels for boxed areas. (G, H) Images show two additional examples of colocalized EGFR and p190RhoGAP on filopodial shafts in FN-adhered cells expressing WT-EGFR. (I) Cells with EGFR (679-AA) adhered to FN for 20 min were stained with phalloidin (green) and antibodies to EGFR (red) and p190RhoGAP (blue). Right, magnified images of individual channels for boxed areas. Arrowheads, lamellipodial cell edge. Scale bars, 10 μm.

contrast, lamellipodial protrusions were devoid of p190RhoGAP at the leading edge in cells expressing EGFR (679-AA) (Figure 4I).

The β3 integrin–EGFR pathway activates p190RhoGAP in mouse mammary epithelial cells with physiological levels of endogenous EGFR

The NR6 heterologous expression system allowed us to hypothesize a role for EGFR in FN-dependent cell adhesion involving activation of the RhoA antagonist p190RhoGAP. This system also identified EGFR (679-AA) as a dominant inhibitory molecule in this pathway. We next sought to confirm and extend these results in normal murine mammary gland (NMuMG) epithelial cells with physiological levels of endogenous EGFR. NMuMG cells expressing recombinant β3 integrin with a D119A mutation that abolishes FN binding and subsequent β3 integrin activation were also examined (Loftus *et al.*, 1994; Galliher and Schiemann, 2006). FN binding induced a robust activation of endogenous EGFR compared with cells kept in suspension (Figure 5A). Endogenous EGFR was also detected in molecular complexes with β3 integrin and p120RhoGAP when parental cells were seeded on FN (Figure 5B). The D119A mutation abolished FN-induced EGFR tyrosine phosphorylation and also prevented EGFR–p120RasGAP complex formation, confirming a role for β3 integrin in the FN–EGFR pathway (Figure 5B). It was not possible to test whether endogenous EGFR recruits p120RasGAP to the plasma membrane using the cell surface coimmunoprecipitation assay due to lack of a suitable mouse-specific EGFR antibody. However, β3 integrin-EGFR-p120RasGAP cell surface complexes were readily detectable using a previously published NMuMG cell line expressing recombinant human

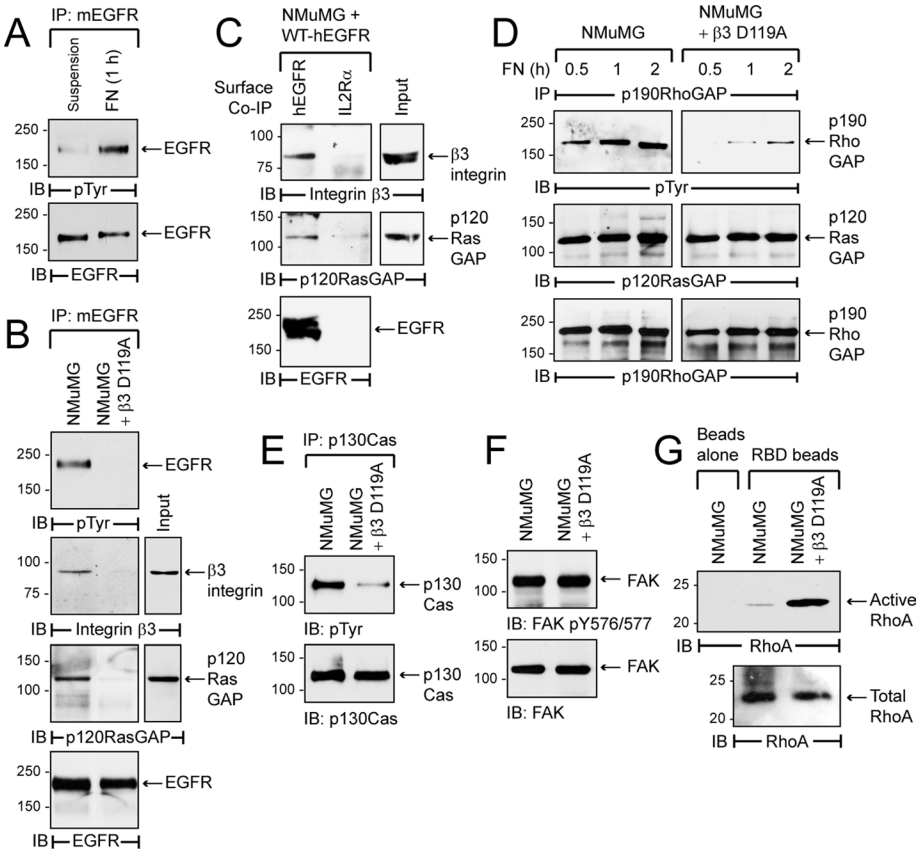

FIGURE 5: β3 Integrin-EGFR cross-talk activates p190RhoGAP in normal mammary gland epithelial cells. (A) Endogenous EGFR immune complexes from NMuMG cells expressing a control EGFP plasmid kept in suspension or adhered to FN for 1 h were immunoblotted with a phosphotyrosine antibody. The same blot was stripped and reprobed with an EGFR antibody. (B) Endogenous EGFR immune complexes from NMuMG cells expressing a control EGFP plasmid or β3 integrin with an inactivating D119A substitution adhered to FN for 1 h were immunoblotted with a phosphotyrosine antibody. The same blot was stripped and reprobed with antibodies to β3 integrin, p120RasGAP, and EGFR. (C) NMuMG cells expressing human EGFR at high levels were incubated with an antibody to an extracellular human EGFR epitope or an isotype-matched negative control (IL2Rα antibody) as they were adhering to FN. Cells were harvested 1 h postadhesion, and immune complexes with membrane-exposed human EGFRs were immunoblotted with an antibody to β3 integrin. The blot was successively reprobed with antibodies to p120RasGAP and EGFR. (B, C) Input lanes are aliquots of total cell protein set aside before immunoprecipitation. (D) p190RhoGAP immune complexes from cells adhered to FN for times indicated were immunoblotted with a phosphotyrosine-specific antibody. Filters were stripped and reprobed with a p120RasGAP antibody and then a p190RhoGAP antibody to control for protein loading. (E, F) Cells adhered to FN for 1 h were harvested to recover p130Cas immune complexes (E) or collect total cellular protein (F). p130Cas immune complexes were immunoblotted with a phosphotyrosine antibody (E) and equal aliquots of total cellular protein blots with a phosphoTyr576/577 FAK antibody (F). Blots were stripped and reprobed with appropriate activation-independent antibodies. (G) Cells were adhered to FN for 1 h, and cell lysates were incubated with glutathione beads alone or glutathione beads loaded with a GST-RBD fusion protein to capture active GTP-RhoA. Bound proteins were immunoblotted with a RhoA-specific antibody (top). Equal aliquots of total cellular proteins were immunoblotted with a RhoA-specific antibody (bottom). Representative of three independent experiments.

EGFR at high levels (Wendt *et al.*, 2010; Figure 5C). These studies were carried out using a monoclonal antibody that specifically recognizes human EGFR. We cannot rule out the possibility that the recombinant human receptor forms a heterodimer with endogenous mouse EGFR following integrin engagement.

There are several different routes linking integrin ligation with Src activity (Huveneers and Danen, 2009). Both FN integrin receptors activate FAK, creating a binding site for Src that subsequently phosphorylates FAK at Tyr576/577 (Calalb *et al.*, 1995). FN binding also induces formation of specific β3 integrin–Src complexes that lead to Src activation (Felsenfeld *et al.*, 1999). We therefore used β3 integrin (D119A) to distinguish between Src substrates modified downstream of these two alternative modes of Src activation. Src-dependent tyrosine phosphorylation of p190RhoGAP was greatly attenuated in cells expressing β3 integrin (D119A) compared with control NMuMG cells (Figure 5D). D119A also interfered with tyrosine phosphorylation of a second FN-dependent Src substrate, p130Cas (Figure 5E). In contrast, FAK underwent Src-dependent phosphorylation in both cell lines, suggesting that this pathway is regulated in part by a β3 integrin–independent mechanism (Figure 5F). The D119A mutation did not completely abolish formation of p120RhoGAP-p190RasGAP complexes, whose assembly is regulated by both phosphotyrosine-dependent and -independent mechanisms (Figure 5D; Roof *et al.*, 1998). However, our data suggest that the D119A substitution results in loss of phosphotyrosine-dependent complex formation required for p190RasGAP activation as a RhoA GAP (Chang *et al.*, 1995; Arthur *et al.*, 2000; Roof *et al.*, 2000; Haskell *et al.*, 2001a, 2001b).

We also demonstrated that FN engagement leads to an initial reduction in GTP-RhoA levels by a mechanism blocked by β3 integrin (D119A) expression using the Rho-binding domain (RBD) of the Rhotekin protein expressed as a glutathione *S*-transferase fusion protein (Figure 5G; Ren *et al.*, 1999). Thus, as in the heterologous expression system, there was a positive correlation between activation of the β3 integrin-EGFR-p190RasGAP pathway and reduced levels of GTP-RhoA in cells with physiological levels of endogenous EGFR.

The β3 integrin–EGFR pathway induces filopodial membrane protrusions in the NMuMG cell model

The next set of experiments tested whether β3 integrin–EGFR signaling was associated with increased membrane protrusive activity in the NMuMG cell model. The cells were first imaged by time-lapse microscopy after FN seeding (Supplemental Video C). Figure 6A shows sequential images from one cell in the video, displaying dynamic growth of a filopodial-like membrane protrusion. Parental NMuMG cells, as well as cells expressing β3 integrin (D119A), were also fixed and costained with phalloidin and a vinculin antibody to image actin cytoskeleton and focal adhesion complexes, respectively, on FN. Similar to NR6 cells reconstituted with human EGFR, the NMuMG cells displayed multiple filopodia, with vinculin staining associated with filopodial actin shafts along with prominent curved stress fibers and a cortical actin filament network (Figure 6B). The D119A substitution was associated

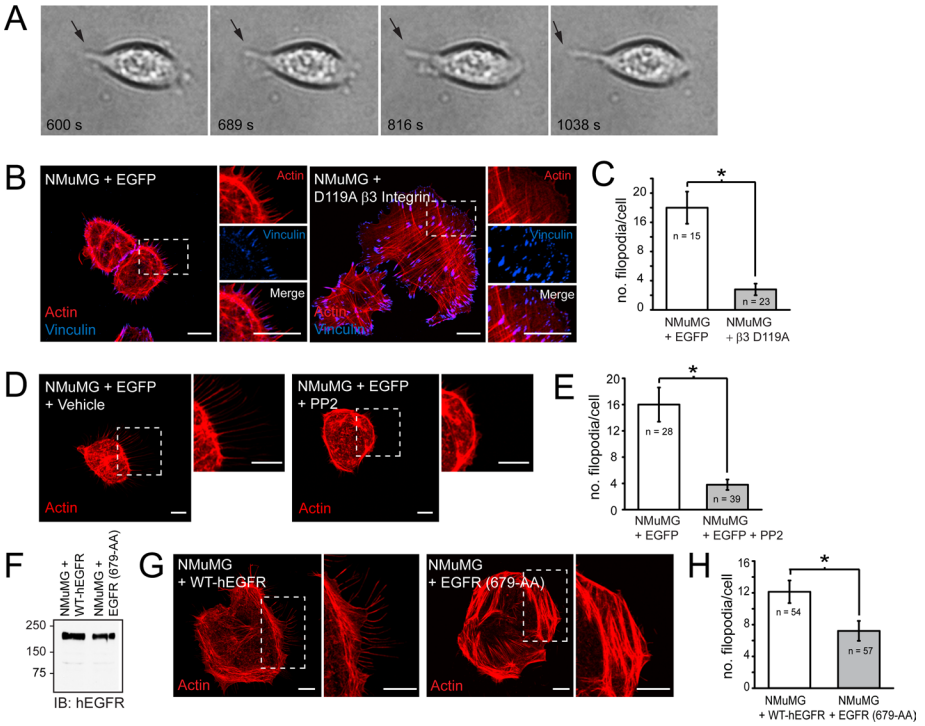

FIGURE 6: β3 Integrin-EGFR interactions induce filopodia membrane protrusions in normal mammary gland epithelial cells. (A) Time-lapse images of NMuMG cell taken from Supplemental Video C starting 600 s after FN seeding. Arrow points to thin structure consistent with filopodia. (B) Confocal images of NMuMG cells with control EGFP plasmid or β3 integrin (D119A) adhered to FN for 1 h stained with phalloidin to visualize actin cytoskeleton (red) and a vinculin-specific antibody (blue). (C) Bars represent the average number of filopodia/cell (mean ± SEM). White bar, control NMuMG cells (n = 15); gray bar, NMuMG cells with β3 integrin (D119A) (n = 23). (D) Confocal images of control NMuMG cells adhered to FN in the absence or presence of Src kinase inhibitor (10 μM PP2) stained with phalloidin (red). (E) Bars represent the average number of filopodia/cell (mean ± SEM). White bars, control NMuMG cells on FN (n = 28); light gray bars, control NMuMG cells on FN in the presence of PP2 (n = 39). (F) Equal total protein aliquots from NMuMG cells with elevated levels of WT human EGFR or EGFR (679-AA) were immunoblotted with a human-specific EGFR antibody. (G) NMuMG cells with elevated levels of human WT-EGFR or EGFR (679-AA) adhered to FN and stained with phalloidin (red). (H) Bars represent the average number of filopodia/cell (mean ± SEM). White bar, NMuMG cells with WT human EGFR (n = 54); gray bar, NMuMG cells with EGFR (679-AA) (n = 57). (C, E, H) Asterisks indicate differences between cells that were statistically significant ($p < 0.001$) as determined by Student's *t* test. (B, D, G) Right, magnified images of individual channels for boxed areas. Size bars, 10 μm. (C, F, H) Representative of two independent experiments.

with a very different phenotype characterized by prominent dorsal stress fibers attached to vinculin-positive focal adhesions at one end (Naumanen *et al.*, 2008; Figure 6B). Cells with β3 integrin (D119A) were also generally devoid of filopodial membrane protrusions, and differences between filopodial formation in these cells versus parental NMuMG cells were statistically significant (Figure 6C). Parental NMuMG cells were also seeded on FN in the presence of PP2 Src kinase inhibitor, which significantly reduced filopodia formation on FN (Figure 6, D and E). Collectively these data support a mechanistic link between β3 integrin, Src kinase, and EGFR and filopodial membrane protrusive activity in a cell model with physiological levels of endogenous EGFR.

EGFR regulates FN-dependent responses in normal breast epithelial cells sensitized for EMT

Although not normally present in the adult mammary tissue, greatly increased FN levels have been found both in development as branching morphogenesis occurs and in various types of mammary tumors (Williams *et al.*, 2008). Given the importance of EMT in normal development and tumor progression we asked whether EGFR signaling has a significant role in normal epithelial cells poised for EMT as they respond to new FN-enriched adhesive environments (Thiery, 2003; Williams *et al.*, 2008). We took advantage of the dominant inhibitory 679-AA mutation identified in the heterologous expression system to test a role for EGFR in the FN-induced phenotype in NMuMG cells. Cells were produced that expressed matched levels of recombinant human WT-EGFR and EGFR (679-AA) (Figure 6F). These cells were then seeded on FN and stained with phalloidin to examine actin cytoskeleton by confocal microscopy. Expression of either form of the EGFR led to increased spread area on FN compared with cells with endogenous receptor (Supplemental Figure S2A). However, filopodia formation was significantly reduced by expression of dominant inhibitory EGFR (679-AA) (Figure 6, G and H). Cells with WT-EGFR also displayed an elongated, mesenchymal-like shape compared with cells with EGFR (679-AA), which were rounded in appearance with broad, lamellipodial membrane protrusions (Supplemental Figure S2, B and C). We used form factor analysis to quantify these differences in cell shape (Mendez *et al.*, 2010). This value varies from 1 to 0, from perfectly circular perimeters to less-rounded perimeters, respectively (Peris *et al.*, 2006). Elongated cells expressing WT-EGFR displayed a low form factor compared with cells with EGFR (679-AA), which had a relatively high form factor (Supplemental Figure S2C). Altogether these data are consistent with the idea that EGFR expressed at high levels plays a role in changes in epithelial cell shape and motility that occur during EMT in FN-rich microenvironments.

DISCUSSION

Prior studies showed that integrin engagement suppresses RhoA activity (Arthur *et al.*, 2000). Src-dependent phosphorylation of p190RhoGAP Tyr1105 creates a binding site for one of the two SH2 domains in p120RasGAP (Hu and Settleman, 1997; Roof *et al.*, 1998). This complex then translocates to the cell surface, where it can down-regulate RhoA via interactions mediated by pleckstrin homology (PH) and/or Ca^{2+}-dependent phospholipid binding (CaLB) domains in p120RasGAP (Gawler *et al.*, 1995; Drugan *et al.*, 2000; Bradley *et al.*, 2006). Our data support an alternative mode of p190RhoGAP membrane translocation involving recruitment of p120RasGAP-p190RhoGAP complexes to activated EGFRs (Figure 7). Similar to EGF stimulation, activated EGFR physically associates with p120RasGAP in response to β3 integrin engagement (Ward *et al.*, 1996). Furthermore, p190RhoGAP colocalizes with EGFR on membrane protrusions. The association between p120RasGAP and EGFR is likely mediated by p120RasGAP SH2 domain binding to a phosphorylated tyrosine residue in EGFR (Wang *et al.*,

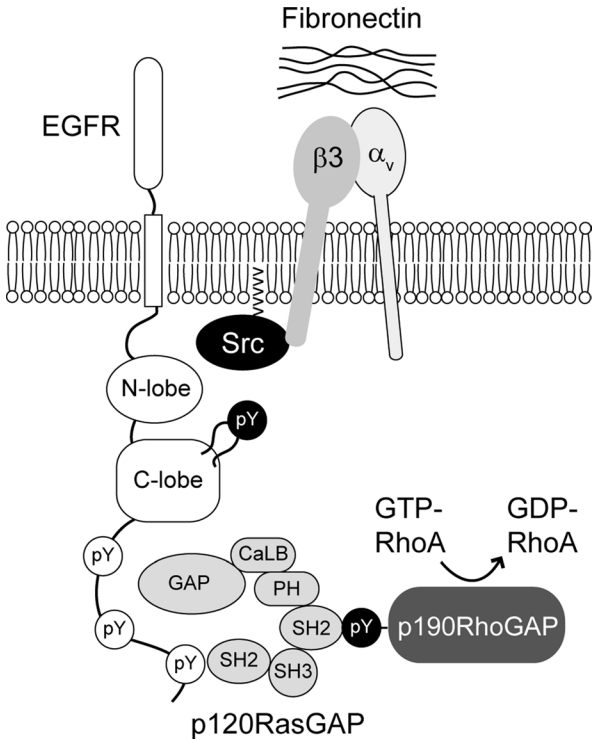

FIGURE 7: Summary model. EGFRs transactivated in β3 integrin complexes are modified at multiple autophosphorylation sites as well as the Src-specific substrate Tyr-845 located in the kinase activation loop (autophosphorylation and Src substrates in white and black, respectively). The β3 integrin engagement is required for Src-dependent phosphorylation of p190RhoGAP leading to its association with a p120RasGAP SH2 domain. Parenthetically, p120RasGAP also has SH3, pleckstrin homology (PH), and Ca^{2+}-dependent phospholipid binding (CaLB) domains in addition to a catalytic GAP domain. EGFR recruits p120RasGAP–p190RhoGAP complexes to plasma membrane, where they may negatively regulate RhoA activity. The EGFR–p120RasGAP association probably involves SH2 binding to an autophosphorylated EGFR tyrosine residue. However, we cannot rule out the possibility that this interaction is mediated by an unknown adaptor molecule.

1996). EGFR Tyr992 can be excluded as a p120RasGAP docking site since it is the only tyrosine phosphorylation event induced by FN binding in EGFR (679-AA) that does not physically associate with p120RasGAP. However, we cannot rule out the possibility that EGFR–p120RasGAP association is mediated by an unknown adaptor protein. EGFR may also synergize with pathways that activate p120RasGAP PH and CaLB membrane docking sites to enhance p190RhoGAP activation.

Active RhoA localizes to the plasma membrane, where it stimulates formation of focal adhesions and stress fibers (Ridley, 2000; Pertz *et al.*, 2006). Previous studies showed that p190RasGAP activation correlates with decreased RhoA activity accompanied by a reduction in stress fiber formation and a corresponding increase in membrane protrusive activity (Arthur *et al.*, 2000; Arthur and Burridge, 2001). However, data obtained using the heterologous NR6 expression system suggest that RhoA down-regulation is not always sufficient to reduce stress fiber formation. It was only when cells were reconstituted with human EGFR that we observed a significant reduction in actin stress fibers, suggesting that EGFR may have a key role in recruiting p190RhoGAP to the plasma membrane, where it can down-regulate RhoA. EGFR expression was also associated with a dramatic increase in filopodia membrane protrusions. Although de novo pathways have been described (Snapper *et al.*, 2001; Czuchra *et al.*, 2005), filopodia usually form by gradual convergence of lamellipodial actin filaments that then elongate from their tips (Svitkina *et al.*, 2003; Yang *et al.*, 2007). The dominant inhibitory 679-AA mutation attenuated filopodia formation and was associated with a dramatic increase in lamellipodia. Our data therefore suggest that EGFR regulates lamellipodia–filopodia transition and that residues Leu-679 and Leu-680 have a positive role in filopodia formation.

EGFR (679-AA) is also tyrosine phosphorylated by FN adhesion but forms a stable complex with β1 integrin instead of β3 integrin. In addition to blocking p190RhoGAP activation, we hypothesize that FN-induced β1 integrin–EGFR (679-AA) complexes sequester one or more components required for EGFR-dependent lamellipodia–filopodia transition, accounting for the phenotype associated with the mutant receptor. However, the mutant receptor is phosphorylated on a single tyrosine residue, suggesting that FN-induced β1 integrin–EGFR (679-AA) complexes probably have restricted signaling capacity. Thus it remains to be seen whether the β1 integrin–EGFR interaction unmasked by the 679-AA mutation is biologically significant. Leu-679 and Leu-680 reside in a region of the EGFR kinase domain with considerable conformational flexibility (Zhang *et al.*, 2006). A rare L679F mutation associated with enhanced EGFR activity in some non–small cell lung cancer patients provides further support that these residues have a critical role in EGFR function (Red Brewer *et al.*, 2009). It is conceivable that EGFR acquires a native conformation involving these residues with a preference for β1 integrin interactions, which could lead to distinct biological outcomes. Of interest, the 679-LL motif is not conserved in other EGFR family members, suggesting that related receptors could evoke distinct cell morphologies and signaling pathways because of preferred binding to different FN receptors (Kil *et al.*, 1999).

The pathway depicted in Figure 7 was also activated in normal mouse mammary gland epithelial cells expressing physiological levels of endogenous EGFR. NMuMG cells with inactive β3 integrin (D119A) displayed prominent dorsal stress fibers and relatively few filopodia compared with parental NMuMG cells, confirming a central role for β3 integrin in the FN–EGFR pathway. Furthermore, FN-activated EGFR was physically associated with p120RasGAP, and p190RhoGAP was specifically activated downstream of β3 integrin–Src signaling. Because the β1 integrin–Src pathway has also been linked to p190RhoGAP activation (Nakahara *et al.*, 1998), our data suggest that there may be subtle differences in spatial or temporal p190RhoGAP regulation, depending on the specific mode of Src activation. Stress fiber reorientation has been linked to mechanosensing at integrin-based focal adhesions (Yoshigi *et al.*, 2005; Hirata *et al.*, 2008). Our data indicate that EGFR–integrin subtype–specific complexes play a role in regulating the type or mode of stress fibers upon FN-dependent adhesion, an important avenue for future study. Previous studies showed that β3 integrin promotes activation of Src that has been "primed" through disruption of intramolecular interactions between a COOH-terminal phospho–Tyr-527 residue and the Src SH2 domain that fold Src into an inactive autoinhibitory conformation (Huveneers *et al.*, 2007). Src autoinhibition can be alleviated by phospho–Tyr-527 dephosphorylation or interaction with a phosphotyrosine residue in another molecule that has a higher affinity for the Src SH2 domain than phospho–Tyr-527 (Hubbard, 1999). In addition to p190RhoGAP, the D119A substitution also attenuated Src-dependent phosphorylation of the p130Cas adaptor protein. Given its involvement in many aspects of adhesion-dependent cell behavior (Defilippi *et al.*, 2006), we cannot exclude the possibility

that p130Cas also contributes to β3 integrin–EGFR signaling. Of interest, p130Cas has been implicated in Src priming by recruiting protein tyrosine phosphatase 1B capable of dephosphorylating phospho–Tyr-527 to p130Cas-Src complexes (Liang *et al.*, 2005). It is conceivable that EGFR also contributes to Src priming.

Mammary gland is an important model of mammalian branching morphogenesis (Gray *et al.*, 2010). Studies employing three-dimensional Matrigel cultures of primary mammary epithelial cells indicate that branching morphogenesis is driven by collective cell migration without formation of leading actin-based membrane protrusions (Ewald *et al.*, 2008). FN appears to have only a moderate effect on mammary gland branching morphogenesis, specifically retarding mammary epithelial cell proliferation (Liu *et al.*, 2010). However, FN undergoes a threefold increase in expression between puberty and sexual maturity and remains high during pregnancy and lactation (Haslam and Woodward, 2003). Furthermore, FN has a critical role in alveologenesis during pregnancy (Liu *et al.*, 2010). Thus β3 integrin–EGFR may regulate formation of filopodia in certain differentiated epithelial cells during postnatal mammary gland development independent of EGFR ligand.

The β3 integrin–EGFR pathway may also have a critical role in human breast cancer since FN is an important component of the tumor microenvironment (Barkan *et al.*, 2010). Mouse mammary epithelial cells with elevated EGFR expression are associated with formation of β3 integrin-EGFR-p120RasGAP complexes at the cell surface, abundant filopodia, and a shift from epithelial toward mesenchymal cell shape downstream of FN binding. Previous studies showed that elevated EGFR expression transforms these cells and also sensitizes them to undergo TGF-β–induced EMT (Wendt *et al.*, 2010). Mouse mammary epithelial cells with elevated expression of the mutant EGFR have reduced numbers of filopodia and lack an elongated mesenchymal appearance. TGF-β induces β3 integrin expression (Galliher and Schiemann, 2006), suggesting that elevated EGFR expression may have a major role in EMT-driven changes in cell shape and motility. In addition, breast cancer has a predilection to metastasize to bone matrix enriched for RGD-containing bone sialoprotein (Sung *et al.*, 1998; Suva *et al.*, 2009). Filopodia regulatory proteins such as Arp2/3, fascin, and Ena/VASP are also associated with increased risk of transformation or metastasis in various cancers when they are expressed at high levels, and many invasive cancer cells have abundant filopodia (Hu *et al.*, 2000; Di Modugno *et al.*, 2006; Vignjevic *et al.*, 2006, 2007; Darnel *et al.*, 2009). Triple-negative breast cancers (TNBCs) have a particularly aggressive phenotype, and EGFR overexpression is associated with poor prognosis in TNBC patients (de Ruijter *et al.*, 2011). TNBC patients do not generally respond to standard EGFR inhibition therapies, which may even exacerbate the disease by selecting for EGFR resistance (Hudis and Gianni, 2011). Further investigation of the β3 integrin–EGFR pathway will help to identify novel molecular targets that drive metastasis in the tumor microenvironment. These future studies will also provide a rationale for development of new therapies that overcome problems associated with EGFR resistance in TNBC and possibly other cancers characterized by EGFR dysfunction.

MATERIALS AND METHODS

Antibodies and reagents

These antibodies were purchased from commercial sources: actin and vinculin mouse monoclonal antibodies from Sigma-Aldrich (St. Louis, MO); FITC-conjugated integrin β1 and β3 antibody and matched FITC-conjugated isotype controls from EBioscience (San Diego, CA); β1 integrin rabbit antibody from Chemicon (Billerica, MA); β3 integrin, FAK, phosphotyrosine, and p130Cas mouse monoclonal antibodies from BD Biosciences (San Jose, CA); mouse-specific EGFR goat and EGFR rabbit antibody from R&D Systems (Minneapolis, MN) and Fitzgerald Industries (Concord, MA), respectively; phospho-EGFR (Tyr-845, Tyr-992, Tyr-1068, Tyr-1173), phospho-FAK (Tyr-397, Tyr-526/527), phospho-p130Cas (Tyr-165, Tyr-249, Tyr-410), and Src rabbit antibodies from Cell Signaling Technology (Beverly, MA); p120RasGAP and p190RhoGAP mouse monoclonal antibodies from Millipore (Billerica, MA); p190RhoGAP rabbit antibody from Bethyl Laboratories (Montgomery, TX); and Rac1 and RhoA rabbit antibodies from Cytoskeleton (Denver, CO). Human-specific EGFR1 mouse monoclonal antibody was produced using the ascites method. All secondary antibodies were purchased from Jackson ImmunoResearch (West Grove, PA). Rhodamine-conjugated phalloidin, Alexa594-wheat germ agglutinin (WGA), and the nuclear counterstain 4′,6-diamidino-2-phenylindole (DAPI) were purchased from Molecular Probes (Eugene, OR). Receptor-grade EGF, selective inhibitors for EGFR (*N*-(3-chlorophenyl)-6,7-dimethoxy-4-quinazolinamine, or AG1478) and Src (4-amino-5-(4-chlorophenyl)-7-(*t*-butyl) pyrazolo-(3,4-d)pyrimidine, or PP2), extracellular matrix proteins, and FITC-conjugated phalloidin were from Sigma-Aldrich, and EM-grade paraformaldehyde from EM Science (Gibbstown, NJ).

Cell lines

NR6 cells are an NIH-3T3 variant lacking endogenous mouse EGFR (Pruss and Herschman, 1977). NMuMG cells are epithelial cells derived from normal mouse mammary gland (David *et al.*, 1981). NR6 cells expressing human WT-EGFR or receptors with 679-LL converted to 679-AA (EGFR (679-AA)), and NMuMG cells with inactive D119A β3 integrin, are described elsewhere (Kil and Carlin, 2000; Galliher and Schiemann, 2006; Kostenko *et al.*, 2006). Permanent NMuMG cell lines expressing WT-EGFR or EGFR (679-AA) were produced using established protocols (Hobert *et al.*, 1997; Wendt *et al.*, 2010). All cells were routinely maintained at 37°C in a humidified atmosphere of 5% CO_2 and 95% air in DMEM supplemented with 10% fetal bovine serum (FBS) and 1% L-glutamine. Media for NMuMG cell lines were additionally supplemented with 10 µg/ml insulin. Cell lines expressing recombinant proteins were selected and maintained in media supplemented with the appropriate antibiotic (G418 [MP Biomedicals, Solon, OH] or puromycin [Invitrogen, Carlsbad, CA]).

Cell adhesion

Cells grown to ~80% confluence were serum starved in media supplemented with 0.5% bovine serum albumin (BSA) and 1% L-glutamine for 5 h and detached from tissue culture plastic with 0.25% trypsin-EDTA. Trypsin was inactivated with a twofold volume of serum-free media supplemented with soybean trypsin inhibitor (0.5 mg/ml; Invitrogen). Cells were allowed to adhere to polystyrene dishes or glass coverslips coated with ECM proteins (10 µg/ml) at a density of ~5×10^4 cells/mm surface area. Control cells were kept in suspension in polystyrene dishes coated with RIA-grade BSA (10 µg/ml).

Analysis of cell spreading

Cells were incubated with Alexa594-WGA and DAPI for 15 min and then fixed with 3% paraformaldehyde–phosphate buffered saline (PBS). Data for mononucleated cells were collected using an Eclipse TE200 microscope (Nikon, Melville, NY) equipped with a digital camera. ImageJ software (National Institutes of Health, Bethesda, MD) was used to quantify the mean surface area per cell based on WGA staining for ≥500 cells in two independent experiments for each cell line. Results are presented as mean surface area (in arbitrary

units [AU])/cell ± SEM as a function of time postadhesion. Surface area adhesion rates (AU/min) were calculated by linear regression analysis for data from the 5, 10, and 20 postadhesion time points.

Confocal and video microscopy

Cells were perforated with 0.5% β-escin in a solution of 80 mM 1,4-piperazinediethanesulfonic acid, pH 6.8, supplemented with 5 mM ethylene glycol tetraacetic acid (EGTA) and 1 mM $MgCl_2$ for 5 min and fixed with 3% paraformaldehyde–PBS for 15 min as described previously (Crooks *et al.*, 2000). Nonspecific binding was blocked with 5% normal serum from the host animal used to generate the secondary antibody. Cells were stained overnight at 4°C or 1 h at room temperature with antibodies diluted in a solution containing 0.5% β-escin and 3% RIA-grade BSA. Confocal images were acquired with a Zeiss LSM 510 Meta laser scanning microscope (Carl Zeiss MicroImaging, Jena, Germany) using diode (excitation 405 nm), Ar (excitation 488 nm), and HeNe (excitation 543 and 633 nm) lasers, 40× or 100× Plan Apo numerical aperture 1.4 objectives, and Zeiss LSM software. For video microscopy, cells were placed in a temperature-controlled chamber at 37°C in an atmosphere of 5% CO_2. Data were analyzed using a Leica 6000 B inverted microscope equipped with a Retiga EXI 12 bit camera (QImaging, Vancouver, Canada) and MetaMorph image analysis software (Molecular Devices, Sunnyvale, CA).

Stress fiber alignment

Stress fiber alignment was carried out using a previously described Sobel filter algorithm to analyze fixed cells stained with rhodamine-conjugated phalloidin (Yoshigi *et al.*, 2003). The Sobel filter algorithm determines the orientation of the pixel intensity gradient in a 3 × 3 pixel area. Images of individual cells were subdivided into 20 × 20 pixel grids, and grids lacking pixels with phalloidin signals were eliminated from the analysis. The average angle of pixel intensity gradient for each grid (i.e., the angle of stress fibers passing the grid) was computed, and the histograms of angle distribution were generated. The kurtosis (i.e., peakedness) of the angle histogram was also determined and defined as "alignment index." Data are presented as mean alignment index ± SEM, n = 100 cells.

Cell morphometry measurements

Quantification of both filopodia and lamellipodia was done using fixed cells stained with rhodamine-conjugated phalloidin. Filopodia were counted using MetaMorph software. Briefly, individual cells were filtered by determining the threshold values for average pixel intensity. The number of filopodia per cell was determined by counting only filopodia with above-average fluorescent intensity following thresholding that crossed the cell edge and were longer than 2 μm. Lamellipodia were quantified using a custom program in the MetaMorph software package that traces and measures the whole-cell perimeter and cell perimeter with adjacent lamellipodial network. The fraction of cell perimeter occupied by lamellipodial network was used as a parameter for quantification. Data are presented as mean number of filopodia/cell, or percentage lamellipodia/cell, ± SEM, n = 60 cells from three independent experiments. The form factor, or $4A\pi/P^2$, where A is the cell area and P is the perimeter, was calculated using the Image Morphometry Analysis feature in MetaMorph software on thresholded cell images.

Cell lysis

Cells were washed three times with PBS supplemented with 5 mM EDTA, 5 mM EGTA, and a phosphatase inhibitor cocktail (10 mM NaF, 10 mM $Na_4P_2O_7$, and 1 mM Na_3VO_4). Cells were lysed with 1% NP-40 in a solution of 50 mM Tris-HCl, pH 8.5, supplemented with 150 mM NaCl, the phosphatase inhibitor cocktail, and a cocktail of protease inhibitors (100 μM phenylmethylsulfonyl fluoride, 10 μg/ml aprotinin, 10 μg/ml leupeptin, 4 μg/ml pepstatin). Cell lysates were clarified by high-speed centrifugation, and protein concentrations were determined by Bradford assay (Bio-Rad, Hercules, CA).

Metabolic labeling

Cells were preincubated in methionine- and cysteine-free medium for 1 h. Amino acid–starved cells were pulse labeled with ^{35}S-Express Protein Labeling Mix (2.5 mCi/ml; PerkinElmer Life Sciences, Boston, MA) diluted in amino acid–deficient medium supplemented with 10% dialyzed FBS and 0.2% BSA for 1 h. The radiolabeled cells were then incubated in chase medium supplemented with a 10-fold excess of nonradioactive methionine and cysteine for 3 h.

Immunoprecipitation and immunoblotting

Conventional immunoprecipitations were carried out by incubating cell lysates with antibodies to specific proteins for 1 h followed by protein A–Sepharose beads (Sigma-Aldrich) for an additional 1 h at 4°C. Surface immunoprecipitations were carried out as described previously (He *et al.*, 2002). Briefly, newly adherent cells were washed with DMEM supplemented with 1% BSA and then incubated with EGFR1 antibody that recognizes an extracellular human EGFR epitope, or an isotype-matched antibody to IL2Rα, diluted in the PBS–BSA solution (10 μl/ml) on ice for 1 h. Cells were washed four times with PBS–BSA, and cell lysates were incubated with protein A beads for 1 h at 4°C to collect immune complexes formed at the cell surface. Immune complexes eluted with sample buffer or equal aliquots of total cellular protein were resolved by SDS–PAGE and transferred to nitrocellulose membranes using standard methods. Blots were blocked in TBS-T (10 mM Tris, 150 mM NaCl, and 0.1% Tween-20) supplemented with 5% nonfat dry milk or 5% BSA. Membranes were incubated with primary antibodies overnight at 4°C, followed by horseradish peroxidase (HRP)–conjugated secondary antibodies for 1 h at room temperature for detection by enhanced chemiluminescence (ECL). ECL signals were quantified using an ImageQuant LAS 4000 digital imaging system and ImageQuant TL software (GE Healthcare, Piscataway, NJ).

Flow cytometry

Cells were trypsinized and either analyzed immediately (EGFR) or following a 3-h incubation in bacterial dishes (β1 and β3 integrins). Cells were stained with primary or secondary antibodies diluted in PBS supplemented with 1% BSA for 30 min on ice, fixed with 2% paraformaldehyde, and analyzed on an iCyte Reflection Flow Cytometer (Champaign, IL).

Rho family GTPase activation assays

GTPase activity was measured using Activation Assay Kits BK036 (Cdc42 and Rac) and BK035 (Rho) from Cytoskeleton according to the manufacturer's instructions. Briefly, cell extracts were prepared with ice-cold cell lysis buffer and immediately snap frozen in liquid nitrogen and stored at −80°C to minimize GTP hydrolysis. An aliquot was set aside for protein concentration determination using the Precision Red Advanced Protein Assay Reagent supplied with the kit. Equal protein aliquots were added to individual wells in an eight-well strip coated with an appropriate RBD, and plates were incubated on an orbital shaker at 4°C for 30 min. Strips were washed and incubated with Rho GTPase–specific primary antibodies, followed by HRP-conjugated secondary antibodies and then an HRP detection reagent supplied with the kit. Absorbance was measured

at 490 nm using a microplate spectrophotometer (SpectraMax 340 Microplate Reader; Molecular Devices). Samples from at least two independent experiments were assayed in triplicate. Data are presented as percentage change relative to cells in suspension ± SEM as a function of time postadhesion. Pulldown assays for active RhoA were carried out with a glutathione *S*-transferase (GST) fusion protein containing the RBD of Rhotekin (gift of Danny Manor, Case Western Reserve University, Cleveland, OH) using established methods (Ren *et al.*, 1999). Briefly, cells were lysed in a solution of 1% Triton X-100, 0.5% sodium deoxycholate, 0.1% SDS, 50 mM Tris-HCl (pH 7.2), 500 mM NaCl, and 10 mM $MgCl_2$ supplemented with protease inhibitors. Clarified lysates were incubated with 10 µg GST-RBD immobilized on glutathione–agarose beads for 90 min at 4°C. Bound proteins were eluted in sample buffer, and RhoA was detected by immunoblotting.

Statistical analyses

Statistical analyses were performed using the Student's *t* test. A p value of <0.001 was considered statistically significant.

Image preparation

Digital images were prepared using Photoshop CS4 and Illustrator CS4 software packages (Adobe, San Jose, CA).

ACKNOWLEDGMENTS

We gratefully acknowledge pilot project support from development funds of the Case Comprehensive Cancer Center Support Grant P30 CA043703. This work was also supported by Public Health Service Grants GM081498 to C.R.C. and CA129359 to W.P.S. N.B. and M.K.W. were supported by fellowships from the National Institutes of Health (HL007653) and the American Cancer Society (PF-09-120-01), respectively. We thank Susann Brady-Kalnay, Meghana Gupta, and members of the Carlin laboratory for many useful discussions.

REFERENCES

Allen FD, Asnes CF, Chang P, Elson EL, Lauffenburger DA, Wells A (2002). Epidermal growth factor induces acute matrix contraction and subsequent calpain-modulated relaxation. Wound Repair Regen 10, 67–76.

Aman A, Piotrowski T (2010). Cell migration during morphogenesis. Dev Biol 341, 20–33.

Arthur WT, Burridge K (2001). RhoA inactivation by p190RhoGAP regulates cell spreading and migration by promoting membrane protrusion and polarity. Mol Biol Cell 12, 2711–2720.

Arthur WT, Petch LA, Burridge K (2000). Integrin engagement suppresses RhoA activity via a c-Src-dependent mechanism. Curr Biol 10, 719–722.

Barkan D, Green JE, Chambers AF (2010). Extracellular matrix: a gatekeeper in the transition from dormancy to metastatic growth. Eur J Cancer 46, 1181–1188.

Barrientos S, Stojadinovic O, Golinko MS, Brem H, Tomic-Canic M (2008). Growth factors and cytokines in wound healing. Wound Repair Regen 16, 585–601.

Bill HM, Knudsen B, Moores SL, Muthuswamy SK, Rao VR, Brugge JS, Miranti CK (2004). Epidermal growth factor receptor-dependent regulation of integrin-mediated signaling and cell cycle entry in epithelial cells. Mol Cell Biol 24, 8586–8599.

Biscardi JS, Maa MC, Tice DA, Cox ME, Leu TH, Parsons SJ (1999). c-Src-mediated phosphorylation of the epidermal growth factor receptor on Tyr845 and Tyr1101 is associated with modulation of receptor function. J Biol Chem 274, 8335–8343.

Borisy GG, Svitkina TM (2000). Actin machinery: pushing the envelope. Curr Opin Cell Biol 12, 104–112.

Bradley WD, Hernandez SE, Settleman J, Koleske AJ (2006). Integrin signaling through Arg activates p190RhoGAP by promoting its binding to p120RasGAP and recruitment to the membrane. Mol Biol Cell 17, 4827–4836.

Calalb MB, Polte TR, Hanks SK (1995). Tyrosine phosphorylation of focal adhesion kinase at sites in the catalytic domain regulates kinase activity: a role for Src family kinases. Mol Cell Biol 15, 954–963.

Carisey A, Ballestrem C (2011). Vinculin, an adapter protein in control of cell adhesion signalling. Eur J Cell Biol 90, 157–163.

Chang JH, Gill S, Settleman J, Parsons SJ (1995). c-Src regulates the simultaneous rearrangement of actin cytoskeleton, p190RhoGAP, and p120RasGAP following epidermal growth factor stimulation. J Cell Biol 130, 355–368.

Chen P, Gupta K, Wells A (1994). Cell movement elicited by epidermal growth factor receptor requires kinase and autophosphorylation but is separable from mitogenesis. J Cell Biol 124, 547–555.

Chou J, Burke NA, Iwabu A, Watkins SC, Wells A (2003). Directional motility induced by epidermal growth factor requires Cdc42. Exp Cell Res 287, 47–56.

Cochet C, Filhol O, Payrastre B, Hunter T, Gill GN (1991). Interaction between the epidermal growth factor receptor and phosphoinositide kinases. J Biol Chem 266, 637–644.

Cohen M, Baum B, Miodownik M (2011). The importance of structured noise in the generation of self-organizing tissue patterns through contact-mediated cell-cell signalling. J R Soc Interface 8, 787–798.

Condeelis J (1997). The biochemistry of animal cell crawling. In: Motion Analysis of Living Cells, ed. D Soll and D Wessels, New York: Wiley-Liss, 85–100.

Countaway JL, Northwood IC, Davis RJ (1989). Mechanism of phosphorylation of the epidermal growth factor receptor at threonine 669. J Biol Chem 264, 10828–10835.

Crooks D, Kil SJ, McCaffery JM, Carlin C (2000). E3-13.7 integral membrane proteins encoded by human adenoviruses alter epidermal growth factor receptor trafficking by interacting directly with receptors in early endosomes. Mol Biol Cell 11, 3559–3572.

Czuchra A, Wu X, Meyer H, van Hengel J, Schroeder T, Geffers R, Rottner K, Brakebusch C (2005). Cdc42 is not essential for filopodium formation, directed migration, cell polarization, and mitosis in fibroblastoid cells. Mol Biol Cell 16, 4473–4484.

Darnel AD, Behmoaram E, Vollmer RT, Corcos J, Bijian K, Sircar K, Su J, Jiao J, Alaoui-Jamali MA, Bismar TA (2009). Fascin regulates prostate cancer cell invasion and is associated with metastasis and biochemical failure in prostate cancer. Clin Cancer Res 15, 1376–1383.

David G, Van der Schueren B, Bernfield M (1981). Basal lamina formation by normal and transformed mouse mammary epithelial cells duplicated in vitro. J Natl Cancer Inst 67, 719–728.

De Luca A, Carotenuto A, Rachiglio A, Gallo M, Maiello MR, Aldinucci D, Pinto A, Normanno N (2008). The role of the EGFR signaling in tumor microenvironment. J Cell Physiol 214, 559–567.

de Ruijter TC, Veeck J, de Hoon JP, van Engeland M, Tjan-Heijnen VC (2011). Characteristics of triple-negative breast cancer. J Cancer Res Clin Oncol 137, 183–192.

Defilippi P, Di Stefano P, Cabodi S (2006). p130Cas: a versatile scaffold in signaling networks. Trends Cell Biol 16, 257–263.

Di Modugno F *et al.* (2006). The cytoskeleton regulatory protein hMena (ENAH) is overexpressed in human benign breast lesions with high risk of transformation and human epidermal growth factor receptor-2-positive/hormonal receptor-negative tumors. Clin Cancer Res 12, 1470–1478.

Drugan JK, Rogers-Graham K, Gilmer T, Campbell S, Clark GJ (2000). The Ras/p120 GTPase-activating protein (GAP) interaction is regulated by the p120 GAP pleckstrin homology domain. J Biol Chem 275, 35021–35027.

Ewald AJ, Brenot A, Duong M, Chan BS, Werb Z (2008). Collective epithelial migration and cell rearrangements drive mammary branching morphogenesis. Dev Cell 14, 570–581.

Felsenfeld DP, Schwartzberg PL, Venegas A, Tse R, Sheetz MP (1999). Selective regulation of integrin–cytoskeleton interactions by the tyrosine kinase Src. Nat Cell Biol 1, 200–206.

Galliher AJ, Schiemann WP (2006). Beta3 integrin and Src facilitate transforming growth factor-beta mediated induction of epithelial-mesenchymal transition in mammary epithelial cells. Breast Cancer Res 8, R42.

Gawler DJ, Zhang LJ, Moran MF (1995). Mutation-deletion analysis of a $Ca^{(2+)}$-dependent phospholipid binding (CaLB) domain within p120 GAP, a GTPase-activating protein for p21 ras. Biochem J 307, 487–491.

Gray RS, Cheung KJ, Ewald AJ (2010). Cellular mechanisms regulating epithelial morphogenesis and cancer invasion. Curr Opin Cell Biol 22, 640–650.

Gupton SL, Gertler FB (2007). Filopodia: the fingers that do the walking. Sci STKE 2007, re5.

Hall JE, Fu W, Schaller MD (2011). Focal adhesion kinase: exploring FAK structure to gain insight into function. Int Rev Cell Mol Biol 288, 185–225.

Haskell MD, Nickles AL, Agati JM, Su L, Dukes BD, Parsons SJ (2001a). Phosphorylation of p190 on Tyr1105 by c-Src is necessary but not sufficient for EGF-induced actin disassembly in C3H10T1/2 fibroblasts. J Cell Sci 114, 1699–1708.

Haskell MD, Slack JK, Parsons JT, Parsons SJ (2001b). c-Src tyrosine phosphorylation of epidermal growth factor receptor, P190 RhoGAP, and focal adhesion kinase regulates diverse cellular processes. Chem Rev 101, 2425–2440.

Haslam SZ, Woodward TL (2003). Host microenvironment in breast cancer development: epithelial-cell-stromal-cell interactions and steroid hormone action in normal and cancerous mammary gland. Breast Cancer Res 5, 208–215.

He C, Hobert M, Friend L, Carlin C (2002). The epidermal growth factor receptor juxtamembrane domain has multiple basolateral plasma membrane localization determinants, including a dominant signal with a polyproline core. J Biol Chem 277, 38284–38293.

Hirata H, Tatsumi H, Sokabe M (2008). Mechanical forces facilitate actin polymerization at focal adhesions in a zyxin-dependent manner. J Cell Sci 121, 2795–2804.

Hobert ME, Kil S, Carlin CR (1997). The cytoplasmic juxtamembrane domain of the epidermal growth factor receptor contains a novel autonomous basolateral sorting signal. J Biol Chem 272, 32901–32909.

Hu KQ, Settleman J (1997). Tandem SH2 binding sites mediate the RasGAP-RhoGAP interaction: a conformational mechanism for SH3 domain regulation. EMBO J 16, 473–483.

Hu W, McCrea PD, Deavers M, Kavanagh JJ, Kudelka AP, Verschraegen CF (2000). Increased expression of fascin, motility associated protein, in cell cultures derived from ovarian cancer and in borderline and carcinomatous ovarian tumors. Clin Exp Metastasis 18, 83–88.

Hubbard SR (1999). Src autoinhibition: Let us count the ways. Nat Struct Biol 6, 711–714.

Hubbard SR (2009). The juxtamembrane region of EGFR takes center stage. Cell 137, 1181–1183.

Hudis CA, Gianni L (2011). Triple-negative breast cancer: an unmet medical need. Oncologist 16 (Suppl 1), 1–11.

Hunter T, Cooper JA (1985). Protein-tyrosine kinases. Annu Rev Biochem 54, 897–930.

Huveneers S, Danen EH (2009). Adhesion signaling—crosstalk between integrins, Src and Rho. J Cell Sci 122, 1059–1069.

Huveneers S, van den Bout I, Sonneveld P, Sancho A, Sonnenberg A, Danen EH (2007). Integrin $\alpha_v\beta_3$ controls activity and oncogenic potential of primed c-Src. Cancer Res 67, 2693–2700.

Hynes R (2002). Integrins: bidirectional, allosteric signaling machines. Cell 110, 673–687.

Jura N, Endres N, Engel K, Deindl S, Das R, Lamers M, Wemmer D, Zhang X, Kuriyan J (2009). Mechanism for activation of the EGF receptor catalytic domain by the juxtamembrane segment. Cell 137, 1293–1307.

Keller R (2005). Cell migration during gastrulation. Curr Opin Cell Biol 17, 533–541.

Kil S, Carlin C (2000). EGF receptor residues Leu^{679}, Leu^{680} mediate selective sorting of ligand-receptor complexes in early endocytic compartments. J Cell Physiol 185, 47–60.

Kil SJ, Hobert ME, Carlin C (1999). A leucine-based determinant in the EGF receptor juxtamembrane domain is required for the efficient transport of ligand-receptor complexes to lysosomes. J Biol Chem 274, 3141–3150.

Kostenko O, Tsacoumangos A, Crooks DM, Kil SJ, Carlin CR (2006). Gab1 signaling is regulated by EGF receptor sorting in early endosomes. Oncogene 25, 6604–6617.

Liang F, Lee SY, Liang J, Lawrence DS, Zhang ZY (2005). The role of protein-tyrosine phosphatase 1B in integrin signaling. J Biol Chem 280, 24857–24863.

Liu K, Cheng L, Flesken-Nikitin A, Huang L, Nikitin AY, Pauli BU (2010). Conditional knockout of fibronectin abrogates mouse mammary gland lobuloalveolar differentiation. Dev Biol 346, 11–24.

Loftus JC, Smith JW, Ginsberg MH (1994). Integrin-mediated cell adhesion: the extracellular face. J Biol Chem 269, 25235–25238.

Maheshwari G, Brown G, Lauffenburger DA, Wells A, Griffith LG (2000). Cell adhesion and motility depend on nanoscale RGD clustering. J Cell Sci 113, 1677–1686.

Maheshwari G, Wells A, Griffith LG, Lauffenburger DA (1999). Biophysical integration of effects of epidermal growth factor and fibronectin on fibroblast migration. Biophys J 76, 2814–2823.

Marcoux N, Vuori K (2003). EGF receptor mediates adhesion-dependent activation of the Rac GTPase: a role for phosphatidylinositol 3-kinase and Vav2. Oncogene 22, 6100–6106.

Martin-Nieto J, Villalobo A (1998). The human epidermal growth factor receptor contains a juxtamembrane calmodulin-binding site. Biochemistry 37, 227–236.

Mattila PK, Lappalainen P (2008). Filopodia: molecular architecture and cellular functions. Nat Rev Mol Cell Biol 9, 446–454.

Mendez MG, Kojima S, Goldman RD (2010). Vimentin induces changes in cell shape, motility, and adhesion during the epithelial to mesenchymal transition. FASEB J 24, 1838–1851.

Moro L *et al.* (2002). Integrin-induced epidermal growth factor (EGF) receptor activation requires c-Src and p130Cas and leads to phosphorylation of specific EGF receptor tyrosines. J Biol Chem 277, 9405–9414.

Muller PAJ *et al.* (2009). Mutant p53 drives invasion by promoting integrin recycling. Cell 139, 1327–1341.

Nakahara H, Mueller SC, Nomizu M, Yamada Y, Yeh Y, Chen WT (1998). Activation of beta1 integrin signaling stimulates tyrosine phosphorylation of p190RhoGAP and membrane-protrusive activities at invadopodia. J Biol Chem 273, 9–12.

Naumanen P, Lappalainen P, Hotulainen P (2008). Mechanisms of actin stress fibre assembly. J Microsc 231, 446–454.

Peris L *et al.* (2006). Tubulin tyrosination is a major factor affecting the recruitment of CAP-Gly proteins at microtubule plus ends. J Cell Biol 174, 839–849.

Pertz O, Hodgson L, Klemke RL, Hahn KM (2006). Spatiotemporal dynamics of RhoA activity in migrating cells. Nature 440, 1069–1072.

Petrie RJ, Doyle AD, Yamada KM (2009). Random versus directionally persistent cell migration. Nat Rev Mol Cell Biol 10, 538–549.

Playford MP, Schaller MD (2004). The interplay between Src and integrins in normal and tumor biology. Oncogene 23, 7928–7946.

Pollard TD, Borisy GG (2003). Cellular motility driven by assembly and disassembly of actin filaments. Cell 112, 453–465.

Pozzi A, Zent R (2011). Extracellular matrix receptors in branched organs. Curr Opin Cell Biol 23, 547–553.

Pruss RM, Herschman HR (1977). Variants of 3T3 cells lacking mitogenic response to epidermal growth factor. Proc Natl Acad Sci USA 74, 3918–3921.

Red Brewer M, Choi SH, Alvarado D, Moravcevic K, Pozzi A, Lemmon MA, Carpenter G (2009). The juxtamembrane region of the EGF receptor functions as an activation domain. Mol Cell 34, 641–651.

Ren XD, Kiosses WB, Schwartz MA (1999). Regulation of the small GTP-binding protein Rho by cell adhesion and the cytoskeleton. EMBO J 18, 578–585.

Ridley A (2000). Rho GTPases. Integrating integrin signaling. J Cell Biol 150, F107–F109.

Roof RW, Dukes BD, Chang JH, Parsons SJ (2000). Phosphorylation of the p190 RhoGAP N-terminal domain by c-Src results in a loss of GTP binding activity. FEBS Lett 472, 117–121.

Roof RW, Haskell MD, Dukes BD, Sherman N, Kinter M, Parsons SJ (1998). Phosphotyrosine (p-Tyr)-dependent and -independent mechanisms of p190 RhoGAP-p120 RasGAP interaction: Tyr 1105 of p190, a substrate for c-Src, is the sole p-Tyr mediator of complex formation. Mol Cell Biol 18, 7052–7063.

Rorth P (2003). Communication by touch: role of cellular extensions in complex animals. Cell 112, 595–598.

Ryan S, Verghese S, Cianciola NL, Cotton CU, Carlin CR (2010). Autosomal recessive polycystic kidney disease epithelial cell model reveals multiple basolateral epidermal growth factor receptor sorting pathways. Mol Biol Cell 21, 2732–2745.

Sander EE, ten Klooster JP, van Delft S, van der Kammen RA, Collard JG (1999). Rac downregulates Rho activity: reciprocal balance between both GTPases determines cellular morphology and migratory behavior. J Cell Biol 147, 1009–1022.

Sato K, Sato A, Aoto M, Fukami Y (1995). c-Src phosphorylates epidermal growth factor receptor on tyrosine 845. Biochem Biophys Res Commun 215, 1078–1087.

Sleeman J, Steeg PS (2010). Cancer metastasis as a therapeutic target. Eur J Cancer 46, 1177–1180.

Snapper SB *et al.* (2001). N-WASP deficiency reveals distinct pathways for cell surface projections and microbial actin-based motility. Nat Cell Biol 3, 897–904.

Sung V, Stubbs JT 3rd, Fisher L, Aaron AD, Thompson EW (1998). Bone sialoprotein supports breast cancer cell adhesion proliferation and migration through differential usage of the alpha(v)beta3 and alpha(v) beta5 integrins. J Cell Physiol 176, 482–494.

Suva LJ, Griffin RJ, Makhoul I (2009). Mechanisms of bone metastases of breast cancer. Endocr Relat Cancer 16, 703–713.

Svitkina TM, Bulanova EA, Chaga OY, Vignjevic DM, Kojima S-I, Vasiliev JM, Borisy GG (2003). Mechanism of filopodia initiation by reorganization of a dendritic network. J Cell Biol 160, 409–421.
Thiery JP (2003). Epithelial-mesenchymal transitions in development and pathologies. Curr Opin Cell Biol 15, 740–746.
Trahey M *et al*. (1988). Molecular cloning of two types of GAP complementary DNA from human placenta. Science 242, 1697–1700.
Tran KT, Griffith L, Wells A (2004). Extracellular matrix signaling through growth factor receptors during wound healing. Wound Repair Regen 12, 262–268.
Vignjevic D, Kojima S, Aratyn Y, Danciu O, Svitkina T, Borisy GG (2006). Role of fascin in filopodial protrusion. J Cell Biol 174, 863–875.
Vignjevic D, Schoumacher M, Gavert N, Janssen KP, Jih G, Lae M, Louvard D, Ben-Ze'ev A, Robine S (2007). Fascin, a novel target of beta-catenin-TCF signaling, is expressed at the invasive front of human colon cancer. Cancer Res 67, 6844–6853.
Wang Z, Tung PS, Moran MF (1996). Association of p120 ras GAP with endocytic components and colocalization with epidermal growth factor (EGF) receptor in response to EGF stimulation. Cell Growth Differ 7, 123–133.
Ward CW, Gough KH, Rashke M, Wan SS, Tribbick G, Wang J (1996). Systematic mapping of potential binding sites for Shc and Grb2 SH2 domains on insulin receptor substrate-1 and the receptors for insulin, epidermal growth factor, platelet-derived growth factor, and fibroblast growth factor. J Biol Chem 271, 5603–5609.
Wels J, Kaplan RN, Rafii S, Lyden D (2008). Migratory neighbors and distant invaders: tumor-associated niche cells. Genes Dev 22, 559–574.
Welsh JB, Gill GN, Rosenfeld MG, Wells A (1991). A negative feedback loop attenuates EGF-induced morphological changes. J Cell Biol 114, 533–543.
Wendt MK, Smith JA, Schiemann WP (2010). Transforming growth factor-beta-induced epithelial-mesenchymal transition facilitates epidermal growth factor-dependent breast cancer progression. Oncogene 29, 6485–6498.
Wiley HS (2003). Trafficking of the ErbB receptors and its influence on signaling. Exp Cell Res 284, 78–88.
Williams CM, Engler AJ, Slone RD, Galante LL, Schwarzbauer JE (2008). Fibronectin expression modulates mammary epithelial cell proliferation during acinar differentiation. Cancer Res 68, 3185–3192.
Wittekind C (2005). Tumours and inflammatory liver diseases. Verh Dtsch Ges Pathol 89, 163–168.
Yang C, Czech L, Gerboth S, Kojima S, Scita G, Svitkina T (2007). Novel roles of formin mDia2 in lamellipodia and filopodia formation in motile cells. PLoS Biol 5, e317.
Yarden Y, Sliwkowski MX (2001). Untangling the ErbB signalling network. Nat Rev Mol Cell Biol 2, 127–137.
Yoshigi M, Clark EB, Yost HJ (2003). Quantification of stretch-induced cytoskeletal remodeling in vascular endothelial cells by image processing. Cytometry A 55A, 109–118.
Yoshigi M, Hoffman LM, Jensen CC, Yost HJ, Beckerle MC (2005). Mechanical force mobilizes zyxin from focal adhesions to actin filaments and regulates cytoskeletal reinforcement. J Cell Biol 171, 209–215.
Zhang X, Gureasko J, Shen K, Cole P, Kuriyan J (2006). An allosteric mechanism for activation of the kinase domain of epidermal growth factor receptor. Cell 125, 1137–1149.
Zhou W, Grandis JR, Wells A (2006). STAT3 is required but not sufficient for EGF receptor-mediated migration and invasion of human prostate carcinoma cell lines. Br J Cancer 95, 164–171.